Scientific Research and Essays Vol. 6(4), pp. 887-895, 18 February, 2011
Available online at http://www.academicjournals.org/SRE
DOI: 10.5897/SRE10.902
ISSN 1992-2248 ©2011 Academic Journals

Full Length Research Paper

A GA-based image alignment approach for tissue image matching

Ting-Hsuan Chen[1]*, Jiun-Hung[1] and Fang-Jung Shiou[2]

[1]Department of Mechanical Engineering, National Taiwan University of Science and Technology, Taipei 10607, Taiwan
[2]Opto-Mechatronics Technology Center, National Taiwan University of Science and Technology, Taipei 10607, Taiwan

Accepted 30 December, 2010

Tissue image matching is important in tissue microarray (TMA) processing, during which massive patient samples are embedded in a single paraffin-based block for simultaneous analysis of pathological features. Prior to TMA processing, the images of the donor block and the corresponding slide must be aligned to determine the desired punching locations. This study developed a genetic algorithm (GA)-based image alignment approach to image superimposition. The similarity between the two images is first evaluated by calculating the dissimilarity area of their binary images using logical operators. The GA is then performed to obtain the optimal translation and rotation parameters for superimposing one image onto another. Experimental results revealed that with both crossover and mutation rates of 0.9, the proposed approach can yield a parameter combination that achieves 100% success of tissue image matching with minimum alignment error.

Key words: Tissue microarray, image alignment, similarity, dismatch factor, genetic algorithm.

INTRODUCTION

Image alignment and image matching are important technologies in machine vision, biomedical imaging and industrial inspection. Hence, image alignment algorithms developed must be efficient, robust and accurate. To meet such requirements, the algorithms have to be executed in a well-controlled environment with constant illumination and fixed working distance between the lens and the object to be inspected. A variety of image alignment techniques have been introduced. They can be separated into two categories, namely intensity-based matching and feature-based matching (Duan et al., 2008; Lai and Fang, 1999).

Intensity-based matching, also known as template matching, involves moving the small reference template within the large scene image on a pixel-by-pixel basis (Chen et al., 2009), followed by calculating the correlation coefficient to determine their similarity. Being simple and easy to program, intensity-based matching can achieve image alignment without feature extraction or direct correspondence between two sets of features. However, changes in illumination during image acquisition may cause variations in intensity value, thus leading to failure in superimposing one image onto another. In other words, intensity-based matching is sensitive to changes in illumination and performs better in a well-controlled environment with constant illumination.

Tsai and Chiang (2002) proposed a wavelet decomposition approach, using pixels and high wavelet coefficient to compute the normalized correlation between images. Tsai and Lin (2003) presented a fast normalized cross correlation to reduce the computational time and to enhance accuracy in defect inspection and measuring surface displacements on mass movements. On the other hand, feature-based matching involves creating a pattern descriptor according to its features, followed by mapping two images together with the feature descriptor. This approach extracts reliable features and robust feature correspondence to overcome outlier problems or missing features. In addition, its performance is not affected by changes in illumination.

Kwon et al. (2001) employed Hausdorff distance matching algorithms using pyramidal structures for image alignment. Li et al. (2003) proposed a new automatic

*Corresponding author. E-mail: d9703201@mail.ntust.edu.tw. Tel: +886-2-27333141, ext. 7348. Fax: +886-2-27376460.

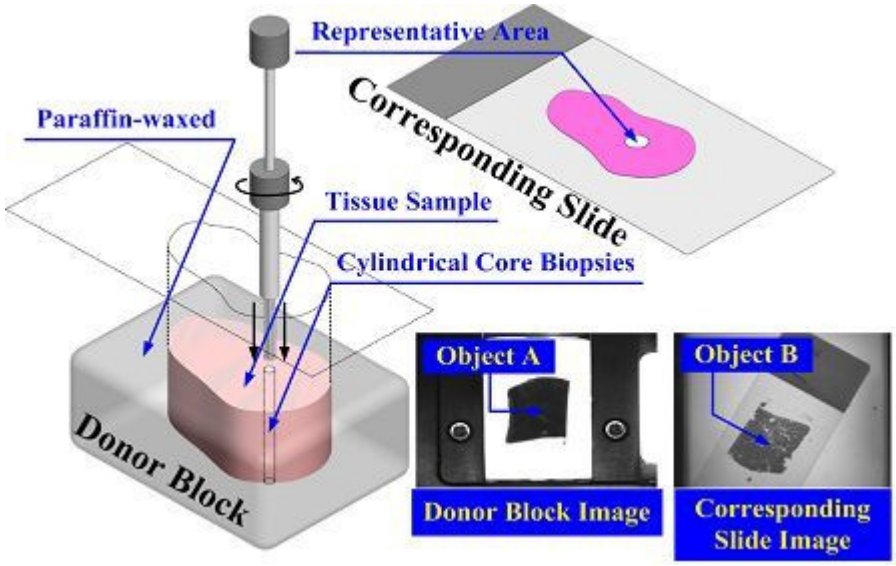

Figure 1. Illustration of tissue image alignment.

invariant feature-based palmprint alignment method for palmprint identification and alignment. Broersen et al. (2008) developed a feature-based image alignment method that used principal component analysis to eliminate image noise for high-resolution imaging mass spectrometry of large biological samples. Figure 1 illustrates the images to be aligned and their sources. As can be seen, one image comes from the donor block where tissue samples taken from organ of donor are embedded in paraffin wax; while the other image comes from the corresponding slide, which is a microscopy glass slide where the tissue slice cut from the donor block is placed. In tissue microarray (TMA) processing, massive cylindrical core biopsies are placed in a single paraffin-based block for simultaneous analysis of pathological features of many patients. The positions where holes are to be punched for extraction of tissues cores are located within the representative area of the corresponding slide. As shown in Figure 1, the images of the donor block (Object A) and the corresponding slide (Object B) must be aligned to determine the desired punching positions.

In the manual approach, a technician or pathologist performs visual alignment under a microscope and points out the desired punching positions (Simon and Sauter, 2002; Parsons and Grabsch, 2009). However, relying on human eyes for performing alignment may lead to errors in positioning and failure in obtaining effective tissue cores. Hence, besides being time-consuming, manual alignment undermines the accuracy of subsequent identification and analysis.

This study developed a genetic algorithm (GA)-based approach for tissue image alignment. A dismatch factor is adopted to measure the similarity of two images. Its value ranges from 0 to 1; and the higher the value, the more similar the two images are. To calculate the dismatch factor, thresholding is performed to obtain their binary images whose respective area is then calculated using logical operators. It is not easy to obtain the best value of dismatch factor by moving randomly the corresponding image according to the translation and rotation parameters.

An optimization approach is thus needed for obtaining an optimum solution. There exists a wide variety of optimization approaches but the common approaches such as gradient method and Newton Method may lead to convergence into local solutions, not to mention the time-consuming calculation they involve. To overcome the drawbacks of optimization approaches, this study applied genetic algorithm (GA) to tissue image matching. Not only can GA avoid local solution, it can also perform efficient and stochastic global search. Experimental results show that GA can obtain optimal translation and rotation parameters for superimposing one image onto another. With both crossover and mutation rates of 0.9, the proposed GA-based image alignment approach has high success rate of image matching and reliable robustness.

GA-based image alignment approach

This section describes the dismatch factor for measuring similarity between images and the GA for searching the best similarity for alignment.

Similarity measurement

Similarity of two images can be measured by superimposing one image onto another. The dismatch factor λ (Bribiesca and Wilson, 1996) for measuring similarity

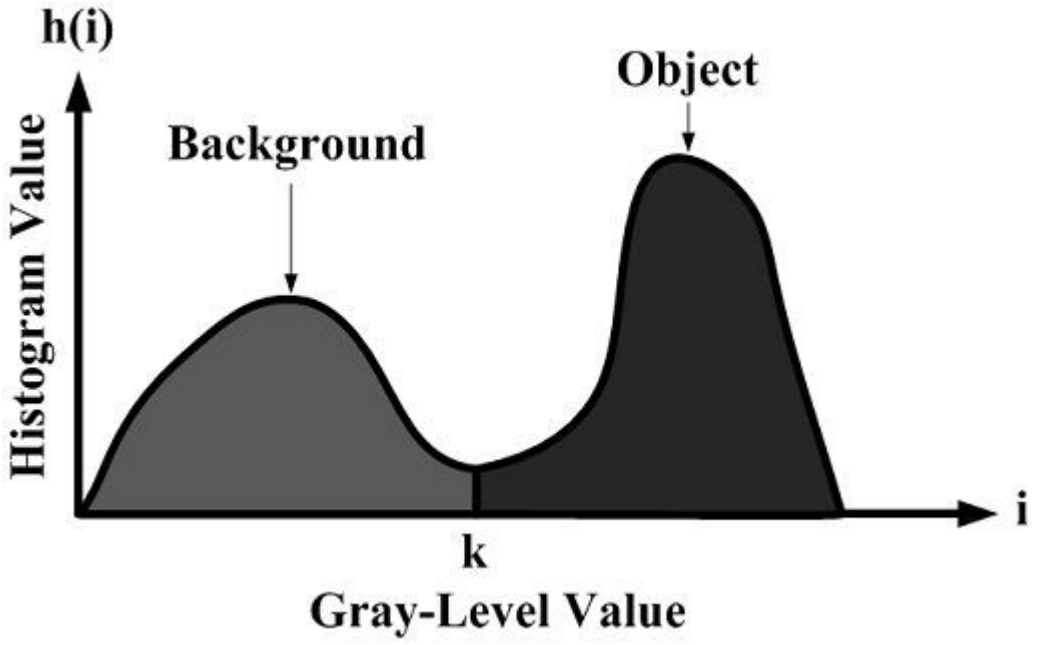

Figure 2. An illustration of a histogram of image for automatic determination of threshold value.

between images A and B ranges from 0 to 1 and can be expressed as follows:

$$\lambda = \frac{y}{x + y} \quad (1)$$

Where x and y denote the area of $A \grave{E} B$ and $A \cdot B$, respectively. The higher the value of λ, the more similar images A and B are.

The areas of A and B and A or B are obtained by performing thresholding to acquire their binary images and then calculating the respective areas using logical operators. Thresholding serves to highlight the feature area in the image. According to the threshold value assigned, the grayscale image inputted will be separated into a binary image containing two regions, namely object and background. The clustering automatic thresholding method (CATM) (National Instrument Corp., 2007) is employed in this study to select automatically threshold value using the histogram of image for distinguishing the tissue from the background.

Figure 2 illustrates a histogram and its parameters, which are used in CATM for automatic selection of threshold value. As can be seen, the x-axis denotes the gray-level value ranging from 0 to 255 while the y-axis denotes the histogram value, which is the number of pixels in the image at each gray-level value. k represents the gray-level value chosen as the threshold value to segment the image into object and background. The value of k can be determined by satisfying the following equation through iterative testing:

$$k = \frac{m_1 + m_2}{2} \quad (2)$$

Where m_1 is the mean of all gray-level values between 0 and k, and m_2 is the mean of all gray-level values between k+1 and 255.

After the binary images are obtained, the logical operators, as shown in Figure 3, are executed to yield the areas of A and B and A or B. The detailed procedures for evaluating similarity can be summarized as follows:

1. Capture the image of the donor block (image A) and the corresponding slide (image B).
2. Execute CATM to determine automatically threshold value k_a and k_b.
3. Perform AND operation on images A and B to produce image C.
4. Calculate the area of image C after AND operation.
5. Perform OR operation on images A and B to produce image D.
6. Calculate the area of image D after OR operation.
7. Substitute values obtained in Steps (4) and (6) into Equation (1) to obtain similarity of images A and B.

Best similarity search

As mentioned above, it is not easy to obtain the best value of dismatch factor by translating and rotating randomly the corresponding image. To overcome the

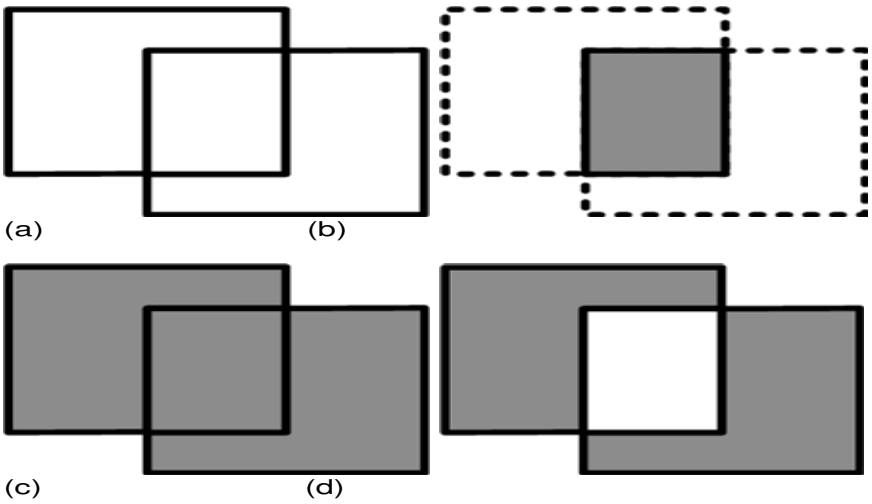

Figure 3. Logical operators: (a) object A and B, ?(b) A and B (c) A or B, and (d) A (And) B/A (or) B

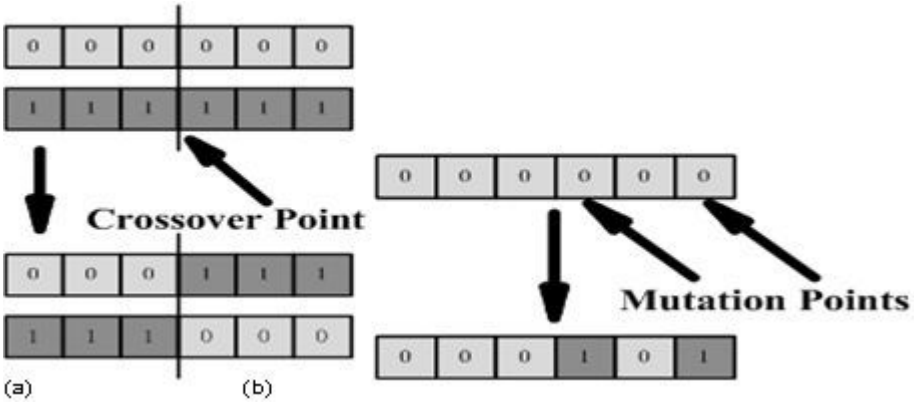

Figure 4. An illustration of GA operators: (a) crossover operation (b) mutation operations.

problem, the GA is adopted to search the best similarity, which represents the greatest fitness value after performing GA under a specific combination. The GA approach is not only feasible but also less time-consuming.

Genetic algorithm – A brief review

Genetic algorithm is a simulation process, which resembles the natural selection of the fittest species for survival. In order to survive and adjust to an unfavorable environment, the species has to evolve into the strongest population. A search by GA involves parallelism and randomization (Goldberg and Holland, 1988). First, GA gathers many binary strings, like chromosomes in biology, into a population, and then performs reproduction, crossover and mutation, thus obtaining the best population. GA has been successfully employed to find acceptable solutions to problems in engineering, business and science. Fitness function provides a standard to evaluate how fit the chromosome is in nature (Unger and Moult, 1993). A higher fitness value implies a better design. The dismatch factor λ used in this study is an example of a fitness function for evaluating the similarity of images with assigned design variable values Δ_x, Δ_y and Δ_α, which are the values of the two translation and one rotation parameters, respectively.

There are three operators, reproduction, crossover and mutation, for manipulating the population to become the strongest one (Deb, 2000; Karhu et al., 2010). These three operators are repeatedly executed to improve the population until no further improvement in fitness is attainable. Reproduction aims to copy old binary strings into the new population according to the fitness value of the binary string. Better fitness value implies greater opportunity to enter the new population. Roulette wheel selection and tournament selection are the most common approaches to selecting excellent genes. Crossover, as illustrated in Figure 4(a) aims to exchange characteristics of binary strings selected from members of the new population.

The crossover rate P_c denotes the number of times the population performs crossover. For example, a 0.5 crossover rate would mean crossover performed 5 times in a population of 10 binary strings or 10 times in a population of 20 binary strings. Mutation, as illustrated in Figure 4(b) aims to prevent a premature

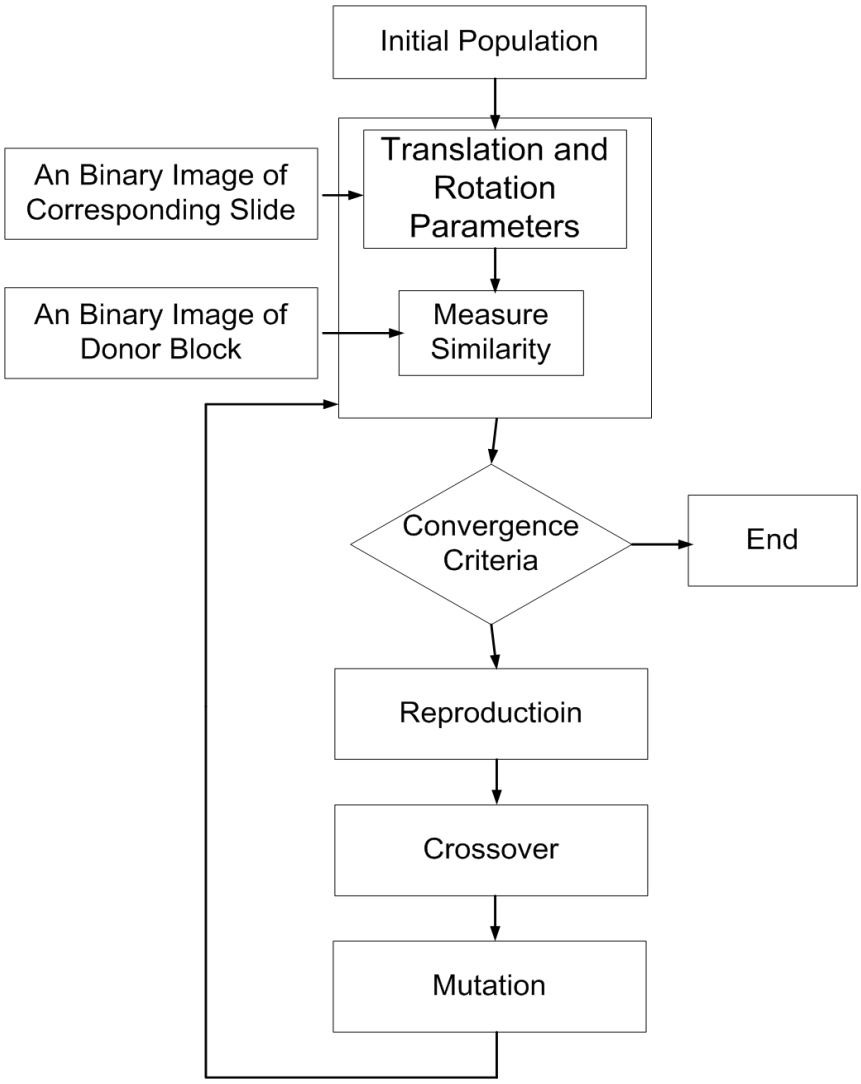

Figure 5. Flowchart for searching best similarity of two images.

loss of valuable binary strings during reproduction and crossover. Similar to crossover rate, mutation rate P_m denotes the number of mutations the population undergoes.

Implementation and procedures

Design variables, fitness function and convergence criteria play important roles when using GA to optimize the desired objective. In this study, the design variables were two translation parameters Δ_x, Δ_y and one rotation parameter Δ_α of the corresponding slide image. When evaluating image similarity, the image of the corresponding slide will be moved. Each design variable is coded in 10 bits, so the total length of the binary string (chromosome) is 30 bits. The resolution of Δ_x, Δ_y and Δ_α are all 0.1 pixel. In addition, the design variable values and the binary strings can be exchanged by the following equation:

$$x = x_{min} + I \frac{x_{max} - x_{min}}{2^L - 1} \quad (3)$$

Where x is design variable value, $[x_{max} - x_{min}]$ is the range of design variable, and I is the integer value of binary string. The range of design variable values for an image of 640*480 pixels can be expressed as follows:

$$\begin{aligned} -640 < \Delta_x < -640 \\ -480 < \Delta_y < -480 \\ 0 < \Delta_\alpha < -360 \end{aligned} \quad (4)$$

Figure 5 shows the flowchart for searching the best similarity of images using GA. As can be seen, the randomly generated initial population with 100 binary strings can first be decoded into 100 design variable values Δ_x, Δ_y and Δ_α. Simultaneously, the binary images of the corresponding slide can be translated and rotated according to the above parameter values. Next, 100 dismatch factor values can be calculated using the binary image of the donor block as well as the translated and rotated images of the corresponding

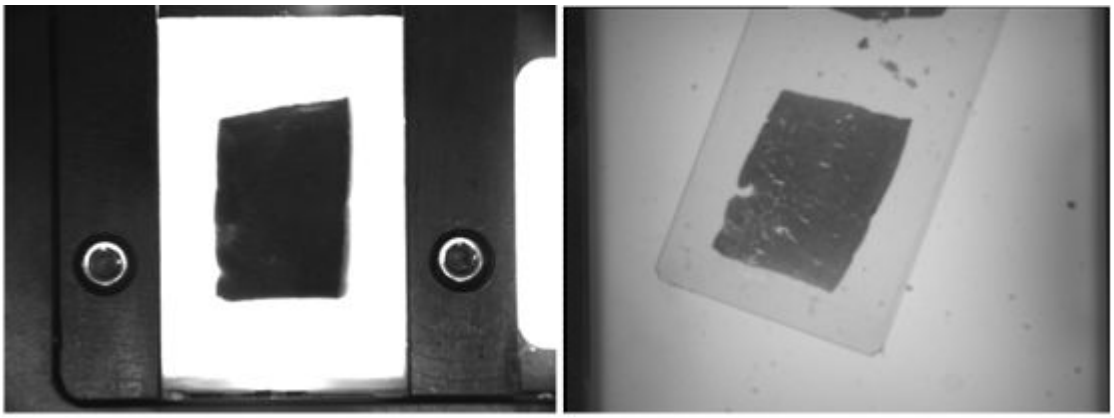

Figure 6. Image of donor block and corresponding slide.

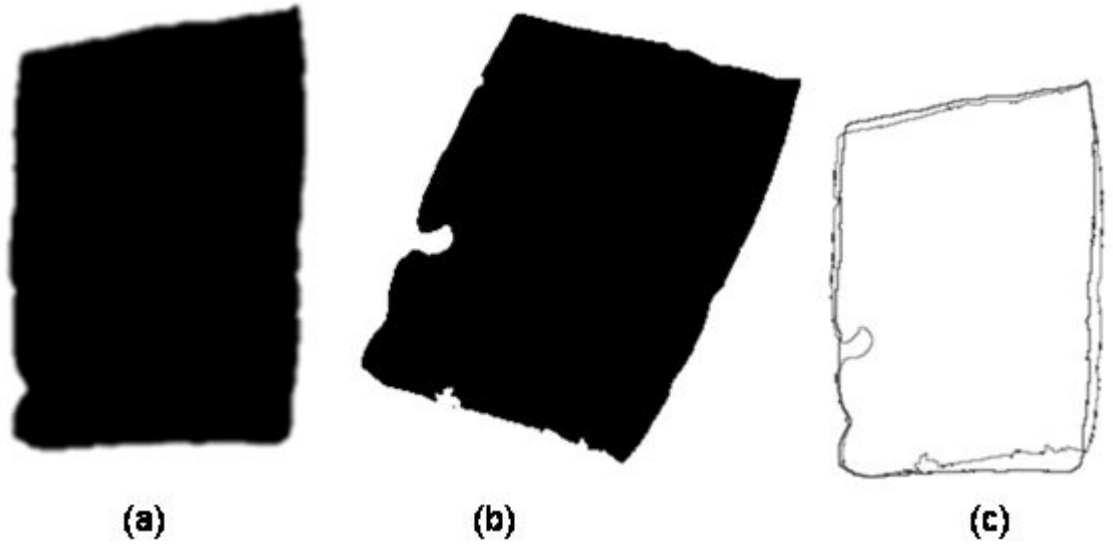

Figure 7. Binary images and image alignment result.

slide. If the convergence criteria are satisfied, the whole process ends and the optimal solution is obtained. Otherwise, the population is manipulated by reproduction, crossover and mutation, followed by re-calculating the dismatch factor values and checking the convergence criteria until the optimal solution is obtained.

RESULTS AND DISCUSSION

Image alignment

Figure 6 shows one of the 10 images of the donor block and corresponding slide. Figures 7(a) and (b) are respectively the binary images of the donor block and corresponding slide, obtained by thresholding the images shown in Figure 6. Figure 7(c) shows the result after GA alignment processing. The image has undergone translation by moving 46 pixels along the x-axis and 2 pixels along the y-axis and rotation by 25° to achieve successful matching with best similarity.

Table 1 shows the alignment results of tissue images of different shapes. The crossover rate is 0.9, the mutation rate is 0.9, and the convergence criterion is 70 iterations. In all 10 experiments, the images of the corresponding slides can be successfully superimposed onto the image of the donor block, as shown in Figure 8.

Robustness

To verify the robustness of the GA-based image alignment approach, the images of the donor block and corresponding slide are aligned 10 times using different combinations of GA parameters. As seen in Table 2, the four combinations are $P_c = P_m = 0.1$, $P_c = P_m = 0.9$, $P_c = P_m = 0.5$. and $P_c = P_m = 0.9$. The differences in design variables values Δ_x, Δ_y and Δ_α under different combinations are calculated using max{1-10}-min{1-10}.

For example, the maximum and minimum of Δ_x

Table 1. Tissue image alignment results.

Exp. NO	Translation and rotation parameters			Similarity	Result
	Δ_x	Δ_y	Δ_α		
1	46	2	25	3.49E-05	Success
2	-10	1	212	3.99E-05	Success
3	-9	7	276	3.58E-05	Success
4	-24	23	89	4.10E-05	Success
5	24	-25	86	4.68E-05	Success
6	5	23	262	4.09E-05	Success
7	-5	-40	162	3.52E-05	Success
8	15	-12	23	3.61E-05	Success
9	10	-23	83	3.78E-05	Success
10	-23	2	257	3.31E-05	Success

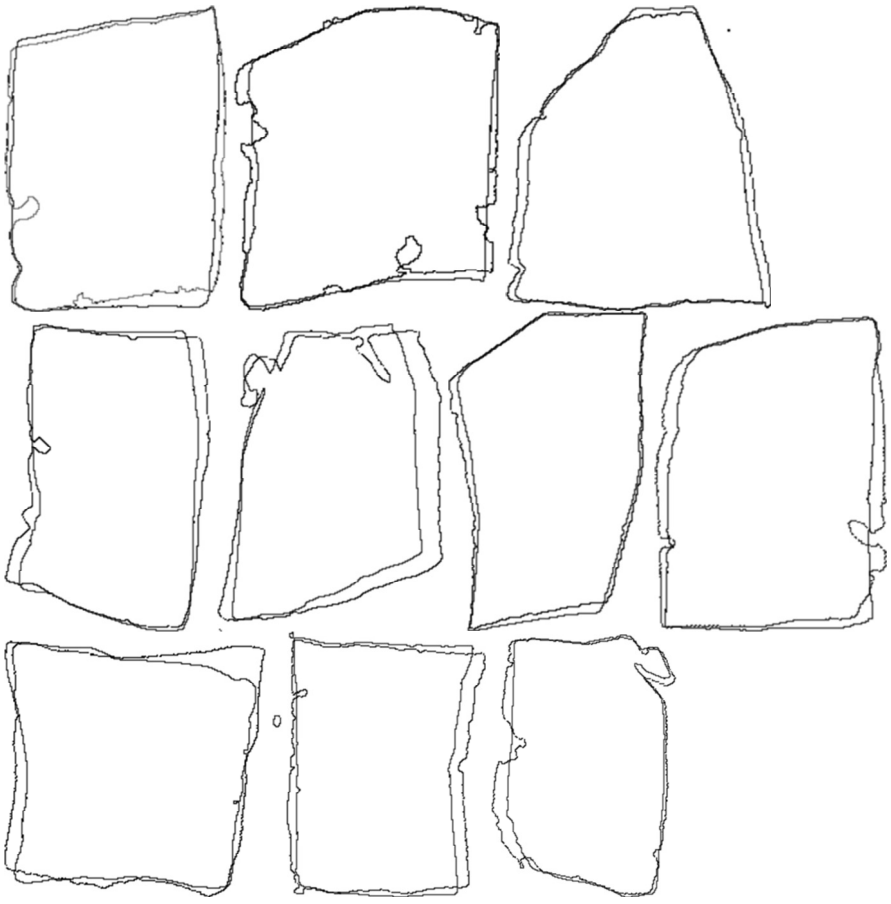

Figure 8. Alignment results of tissue images of different shapes.

unde $P_c = P_m = 0.1$ are 21 and -13, respectively. Thus, the difference of Δ_x under $P_c = P_m = 0.1$. is 21-(-13) = 34. The results show that when the crossover rate and mutation rate are both 0.9, the difference in Δ_x, Δ_y and Δ_α are only 5 pixels, 7 pixels and 10°, respectively; indicating success in image matching with best similarity achieved by parameter combination of $P_c = P_m = 0.9$.

Figure 9 shows the success rate of tissue image matching under different parameter combinations. As can be seen, the four combinations achieve a success rate of

Table 2. Robustness achieved under different parameter combinations

Trials	$P_c = P_m = 0.1$			$P_c = P_m = 0.3$			$P_c = P_m = 0.5$			$P_c = P_m = 0.9$		
	Δ_x	Δ_y	Δ_α	Δ_x	Δ_y	Δ_α	Δ_x	Δ_y	Δ_α	Δ_x	Δ_y	Δ_α
1	-7	4	213	-10	1	212	18	-6	33	-10	1	212
2	-9	3	210	-15	0	211	18	-5	33	-7	3	212
3	19	-9	36	-9	-3	213	-10	1	212	-10	0	211
4	-9	1	212	18	0	32	18	-6	33	-7	3	211
5	-11	8	214	-10	0	212	18	-6	34	-12	6	212
6	18	-3	34	-13	3	211	-10	1	212	-10	0	212
7	17	-6	33	19	-6	34	-4	-4	209	-10	-1	206.
8	18	-5	33	18	-6	34	-16	-1	208	-11	-1	213
9	-13	-2	211	-11	4	217	-11	1	213	-7	2	216
10	21	-13	37	-11	2	214	-10	1	212	-7	3	211
Difference*	34	21	181	34	10	185	34	7	180	5	7	10

* The difference is calculated by max (1-10)-min(1-10).

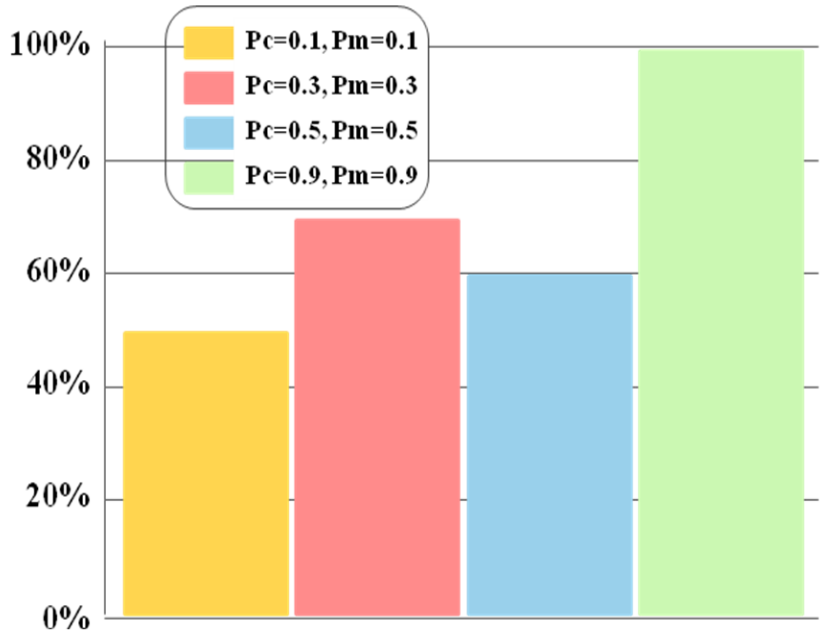

Figure 9. Success rate of tissue image matching under different parameter combinations.

50, 70, 60 and 100%, respectively, revealing successful image superimposition under 0.9/0.9 crossover/mutation rate with 100% success under parameter combination of $P_c = P_m = 0.9$.

DISCUSSION

The experimental results not only show high success rate of tissue image matching but also best similarity of images achieved under parameter combination of $P_c = 0.9$ and $P_m = 0.9$. In other words, the proposed GA-based image alignment approach is both feasible and reliable for tissue image matching. Difference between an image of the donor block and that of the corresponding slide can be attributed to the following factors. First, shape difference between the original tissue sample and its tissue sections may arise as a result of shrinkage in the section sampled by the skilled technician. Second, image difference occurs as an error of the image alignment approach. Third, vibration and unstable illumination during image acquisition may result in distorted image

captured. To maintain good reliability of the proposed image alignment approach, the above must be avoided as far as possible.

Conclusion

This study developed a GA-based image alignment approach that uses the dismatch factor to measure similarity for tissue image matching. Experimental results evidence its high success rate of image matching and reliable robustness. Hence, the proposed approach offers an alternative method for determining desired punching positions in TMA processing.

References

Bribiesca E, Wilson RG (1996). A measure of 2D shape-of-object dissimilarity. Appl. Math. Lett., 10(6): 107-115.

Broersen A, Liere RV, Altelaar AFM, Heeren RMA, McDonnell LA (2008). Automated, feature-based image alignment for high-resolution imaging mass spectrometry of large biological samples. Am. Soc. Mass Spectrom., 19: 823-832.

Chen CS, Yeh CW, Yin PY (2009). A novel Fourier descriptor-based image alignment algorithm for automatic optical inspection. J. Visual Commun. Image Rep., 20: 178-189.

Deb K (2000). An efficient constraint handling method for genetic algorithms. Comput. Methods in Appl. Mech. Eng., 186: 311-338.

Duan W, Kuester F, Gaudiot JL, Hammami O (2008). Automatic object and image alignment using Fourier descriptors. Image and Vision Comput., 26: 1196-1206.

Goldberg DE, Holland JH (1988). Genetic algorithms and machine learning. Machine Learn. 3: 95-99.

Karhu K, Khuri S, Makinen J, Tarhio J (2010). Identifying human miRNA targets with a genetic algorithm. Assoc. Comput. Mach., pp. 15-17.

Kwon OK, Sim DG, Park RH (2001). Robust Hausdorff distance matching algorithms using pyramidal structures. Pattern Recognition., 34: 2005-2013.

Lai SH, Fang M (1999). Robust and efficient image alignment with spatially varying illumination models. IEEE Computer Society Conference on Computer Vision and Pattern Recognition. Fort Collins, CO.

Li W, Zhang D, Xu Z (2003). Image alignment based on invariant features for palmprint identification. Signal Processing: Image Commun., 18: 373-379.

National Instrument Corp. (2007). NI Vision Concepts Manual. National Instrument Corp., Austin, Texas, pp. 8.1-8.9.

Parsons M, Grabsch H (2009). How to make tissue microarrays. Diagnos. Histopathol., 15(3): 142-150.

Simon R, Sauter G (2002). Tissue microarrays for miniaturized high-throughput molecular profiling of tumors. Exp. Hematol., 30: 1365-1372.

Tsai DM, Chiang CH (2002). Rotation-invariant pattern matching using wavelet decomposition. Pattern Recognition Letters., 23:191-201.

Tsai DM, Lin CT (2003). Fast normalized cross correlation for defect detection. Pattern Recognition Lett., 24: 2625-2631.

Tsai DM, Lin CT, Chen JF (2003). The evaluation of normalized cross correlations for defect detection. Pattern Recognition Lett., 24:2525-2535.

Unger R, Moult J (1993). Genetic algorithms for protein folding simulations. J. Mol. Biol., 231:75-81.